

ORIGINAL

Open Access

Study of influential factors in synthesis and characterization of cobalt oxide nanoparticles

Ghazaleh Allaedini* and Abubakar Muhammad

Abstract

This study has investigated the different factors in obtaining cobalt oxide nanoparticles. The factors that have been studied are the effect of pH, synthesis temperature, capping agent, annealing temperature, and different usage of cobalt salts. Cobalt oxide nanoparticles were characterized by scanning electron microscopy, energy dispersive X-ray spectroscopy, UV, Fourier transform infrared spectroscopy, and X-ray diffraction. In order to find the effects of various factors, the optimum pH was achieved in the first experiment by the precipitation method; after finding out that in experiments with pH 8 to 9, the particles are homogeneous in shape and regular. The other experiments were repeated with the same pH but changing the factors. In the second experiment, the effect of synthesis temperature at 40°C, 60°C, 80°C, and 100°C was investigated. To find out the effect of capping agent, two experiments were done, one using the oleic acid and the other using 2-(dodecyloxy) acetic acid. In the case of investigating the annealing temperature, the black cobalt oxides were annealed at 400°C, 500°C, and 600°C. The last one was done using two different cobalt salts, cobalt nitrate and cobalt sulfate. Finally, cobalt oxide nanoparticles were characterized.

Keywords: Cobalt oxide nanoparticles; Co-precipitation method; pH effect; Synthesis temperature; Capping agent; Annealing temperature; Cobalt salt type

Background

Cobalt-based nanoparticles reside among the most promising materials for technological applications like information storage devices, magnetic fluids, and catalysts [1]. Co is a well-known ferromagnetic material which is commonly used as an alloying element in permanent magnets. It exists in two forms: hexagonal close packed (HCP) and face-centered cubic (FCC). HCP is the stable phase at room temperature, whereas FCC is stable at temperatures above 450°C [2]. Nanosized Co particles display a wide range of interesting size-dependent structural, electrical, magnetic, and catalytic properties [3]. In particular, because of their large surface area, Co nanoparticles showed high chemical reactivity, which makes them suitable for catalysis [4]. To have further applications of cobalt in different industries such as separation technology, information storage systems, catalysis, and biomedicine [5], nanoparticles are required to be discrete, identical in size and shape, and uniform in composition and crystal structure [6]. Thus, characterization

should be done to have a broad knowledge on cobalt oxide nanoparticles. In this study, the different factors have been investigated to see their effects on the structure and morphology of cobalt oxide nanoparticles.

Results and discussion

Effect of pH

Scanning electron microscopy (SEM) images of Co_3O_4 synthesized by suspension at pH 8 to 10 in a co-precipitation reaction are shown in Figure 1. Comparing them, we see that nanocubic Co_3O_4 with the average particle size of 20 nm is formed when pH is 8 to 9, and when pH increases at 10 to 11, some irregular Co_3O_4 including the grains that are recombined in the products are formed. This fact can be explained as the condensation reaction of $\text{Co}(\text{OH})_2$ precursors is able to happen at higher pH value, and agglomeration of the nanoparticles occurs. The average sizes of nanoparticles were calculated to be 20 nm at pH 8 to 9 and 30 nm at pH 10 to 11 using Debye-Scherrer's equation. At pH 9 to 10, some areas with distorted strings can be seen due to self-alignment orientation that has

* Correspondence: jiny_ghazaleh@yahoo.com
Chemical Engineering Department, UKM, Bangi, Selangor, Malaysia

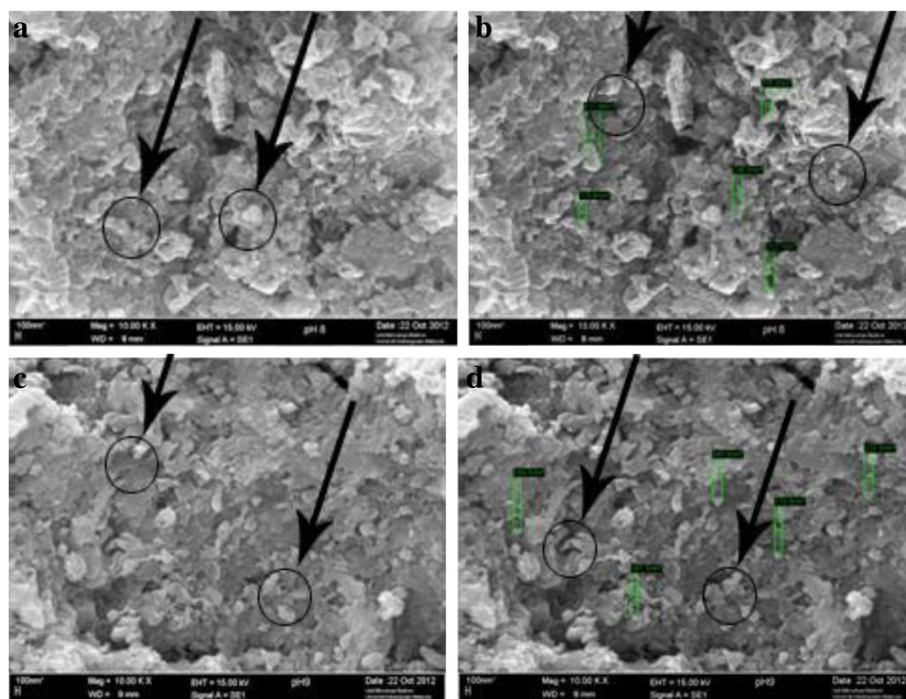


Figure 1 SEM images at pH 8 (a, b) and pH 9 (c, d).

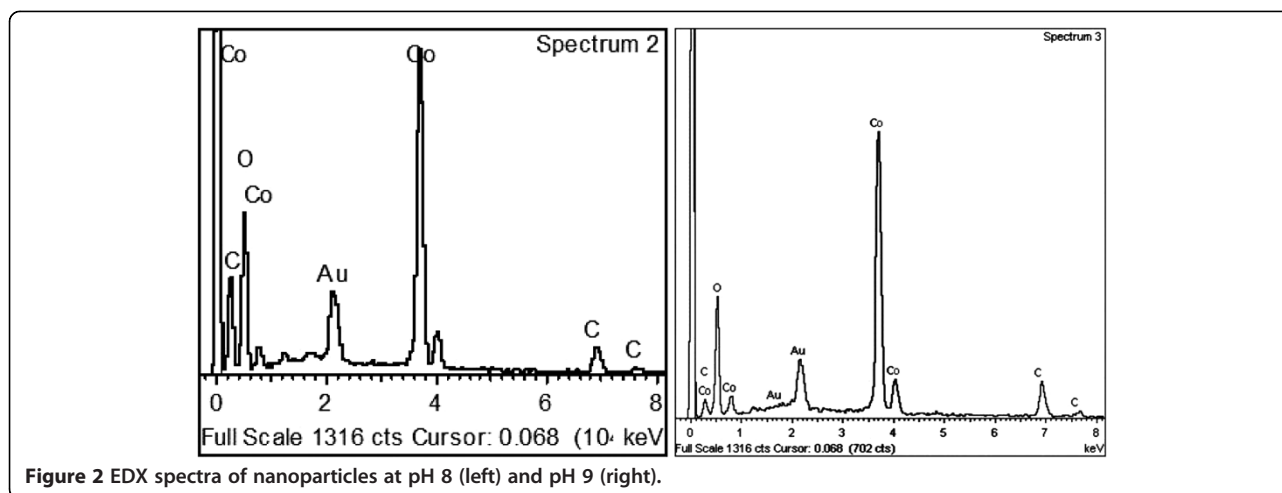
happened, and this can be attributed to the presence of weak interactions. However, the crystalline Co_3O_4 nanoparticles can be observed as crystals in some areas of the micrographs. The pH range of 8 to 9 makes more uniform and smaller nanoparticles than pH 10 to 11. Large and agglomerated particles have been synthesized at higher pH since the nucleation rate is lower than the particle growth rate. Higher pH range increases synthesis rate; thus, the produced cobalt sample will be non-uniform and agglomerated. The obtained results show that the solution pH of 8 to 9 is a better one to synthesize uniform cobalt since at lower pH, condensation reaction was considerable so that the cobalt sample was completely agglomerated (Table 1). At higher pHs (10 to 11), reduction rate of Co ions was fast so that obtained samples were agglomerated less and a bit without any nanorods. In Figure 2, energy dispersive X-ray spectroscopy (EDX) spectra are shown.

Table 1 Weight and atomic percentages at pH 8 and 9

	Weight percentage (pH 8)	Atomic percentage (pH 8)	Weight percentage (pH 9)	Atomic percentage (pH 9)
CK	22.95	34.87	6.35	11.63
OK	45.73	52.15	48.16	66.22
CoK	22.49	10.24	29.43	16.15
NaK	8.83	2.73	16.07	6.00
Total	100	100	100	100

Identification was done by comparing the diffraction patterns with the standard X-ray diffraction pattern of the synthesized cobalt oxide that was analyzed to investigate the phase structure and the crystallinity which is shown in Figure 3. The patterns show sharp peaks relating to and according to standard Co_3O_4 X-ray diffraction (XRD) pattern (Joint Committee on Powder Diffraction Standards (JCPDS) no. 43–1003). All the peaks of cobalt oxide can be indexed to cubic phase.

Figure 3 shows a crystalline Co_3O_4 with small broadened profiles of all measured reflections and a crystalline powder which has sharp and a kind of intense diffraction peak. There are no impurity peaks, and this fact shows that the final product synthesized is Co_3O_4 with nanocubic structure by co-precipitation. In addition to the facts mentioned, the XRD patterns show the crystalline phase, and they are in agreement with reported values of selected area electron diffraction (SAED) pattern that shows the presence of well-defined clear spot. However, for pH 10 to 11, it has some broad diffraction lines which remind some inefficient crystallinity. Even if we look at the images of SEM (Figure 4), we can see some spherical agglomeration with some pores. The XRD plot of the cobalt powder at pH 8 to 9 shows the presence of both HCP and FCC phases. Also, the allotropic transition from HCP to FCC phase happened as the pH changes. The peak broadening at each reflection is also indicative of the formation of fine size cobalt powder.



When the pH lies in the range of 8 to 9, Co_3O_4 dominates the product in the XRD pattern (Figure 5). At pH 10 to 11, a weak diffraction peak of CoO is observed. A small amount of cubic Co_3O_4 is found at pH 10 to 11 (Table 2). Based on Scherrer's formula, the average particle sizes of Co_3O_4 at pH 8 to 9 are 40 and 50 nm. Co_3O_4 gave the large crystallite size because it contains three Co ions which have large radii (Table 3). At pH 10 to 11, the range is 20 to 30 nm. The crystallite sizes were calculated using XRD data based on Debye-Scherrer's equation as follows:

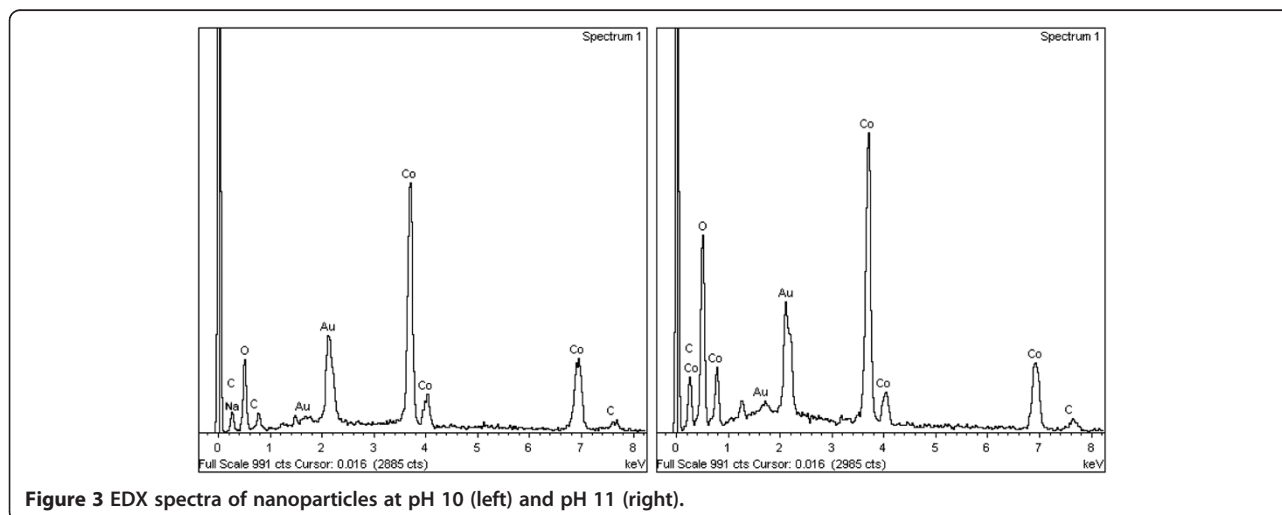
$$d = \frac{0.89 \lambda}{\beta \cos \theta}$$

where d , λ , θ and β are the crystallite size, X-ray wavelength (1.542 Å), Bragg diffraction angle, and full width at half maximum (FWHM) of the diffraction peak. After

drying in an inert atmosphere at pH 8 to 9, a change from amorphous to crystalline state can be seen.

This shows narrow particle size distribution in a well-defined particle size, purity of the phase, and the structure and shape. A stretching frequency at 3,361.2 cm^{-1} and a weak asymmetric band at 2,919 cm^{-1} will prove the existence of OH group due to the absorption of water by nanoparticles during sample preparation (Figure 6). The presence of two strong M-O stretching and bending frequencies at 1,481 and 831 cm^{-1} shows phase purity of monodisperse one in the face-centered cubic structure. The peaks at 1,579 and 1,539 cm^{-1} correspond to Co_3O_4 asymmetric stretching vibrations. The peak at 3,610 cm^{-1} corresponds to CoO bending vibrations at pH 11.

The optical property of cobalt oxide nanoparticle has been found with high purity, and the crystallinity of the cobalt oxides were confirmed with the help of UV-visible absorption spectra by observing the absorption rate



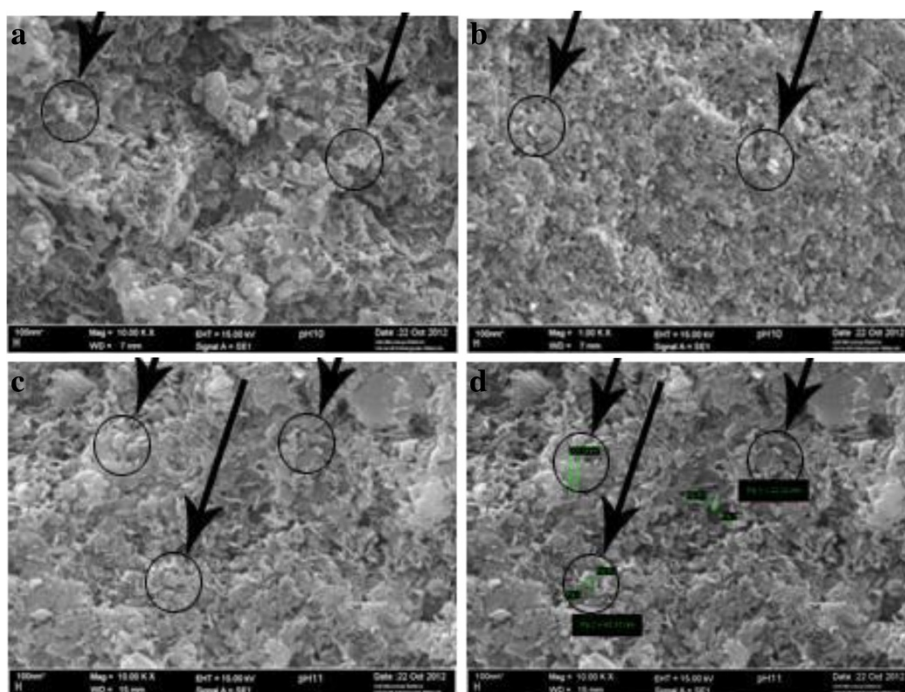


Figure 4 SEM images at pH 10 (a, b) and pH 11 (c, d).

band at 210 nm with a tail which is extended towards a longer wavelength (Figure 7), and the reason for that is their quantum size effects. In the extending tail, there is no significant absorption peak due to quantum confinement effects in the energy gap. The absorption peak is a bit broad peak due to the particle size. CoO nanoparticles are considered as stable, and this fact can

be the result of symmetrical polarity structure which depends on the weak interaction of van der Waals forces within the particle regime.

Effect of synthesis temperature

Four samples were synthesized at different temperatures. The prepared samples were characterized by SEM.

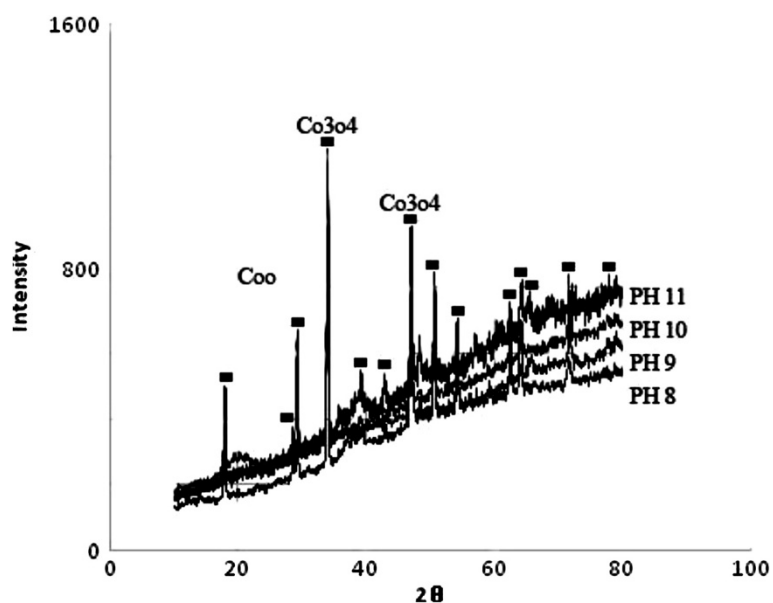


Figure 5 XRD patterns of cobalt oxide nanoparticles at different pHs.

Table 2 Weight and atomic percentages at pH 10 and 11

	Weight percentage (pH 10)	Atomic percentage (pH 10)	Weight percentage (pH 11)	Atomic percentage (pH 11)
CK	10.62	22.46	14.90	25.63
OK	29.14	46.29	43.97	56.77
CoK	26.05	16.51	19.30	9.95
NaK	34.20	14.74	21.83	7.65
Total	100	100	100	100

Figure 8a, b, c, d shows the SEM images of the cobalt samples which were synthesized at 40°C, 60°C, 80°C, and 100°C, respectively. When the reaction was performed at a temperature lower than 60°C, the reaction rate was very slow, and the prepared sample was amorphous and agglomerated. At temperatures higher than 60°C, the synthesis rate is fast, but the prepared samples showed that the higher temperature causes more agglomeration. Amorphous percentage of samples is increased because, at high reaction rate, nucleation and particle growth processes are not controllable. This fact can be concluded in figure 9 showing the EDX too. They were analyzed by XRD. Figure 10 shows the XRD patterns of these samples. As can be seen from the figure, the solution temperature has an important role in the composition and phase control of the synthesized sample. At 60°C and lower, pure metallic cobalt can be synthesized. At high temperatures, 80°C and more, cobalt will be formed in oxide forms such CoO, Co₂O₃, and CoO₂. Based on XRD results, the metallic cobalt content of samples is decreased when the synthesis temperature is increased from 40°C up to 100°C and more. However, the combination of SEM and XRD results for temperature studies shows that the sample

Table 3 Crystallite size and particle size found by Scherrer

pH	Crystallite size (nm)	Particle size (nm)
8	3.22	40
9	3.25	50
10	4.75	20
11	4.89	30

synthesized at 60°C has uniform morphology, small particles, and composition without any impurity. The comparison is even possible through the peaks at FTIR in Figure 11.

Effect of annealing temperature

Figure 12 shows X-ray diffraction patterns of Co₃O₄ at different annealing temperatures of 400°C, 500°C, and 600°C; small peaks were observed, and a poor crystallinity at 400°C is shown. The ones annealed at temperature more than 500°C exhibit sharp diffraction peak characteristics of the Co₃O₄ cubic spinel structure. From Figure 12, phases ($2\theta \approx 22.90^\circ$), ($2\theta \approx 35.80^\circ$), ($2\theta \approx 58.20^\circ$), and ($2\theta \approx 78.10^\circ$). XRD peaks were observed at the temperature of 600°C, and it is concluded that all of them were crystalline with a cubic spinel structure (JCPDS) and a random orientation, which generally occurs in the growth of Co₃O₄. The degree of orientation of the Co₃O₄ was strongly dependent on the annealing temperature. It increases as the annealing temperature increases. The average particle sizes of Co₃O₄ thin film were calculated using the full width at oxygen defects at the grain boundaries. As a result, these defects are favorable to the merging process to form larger Co₃O₄ grains while increasing the annealing temperature. As the annealing temperature increases from 400°C to 600°C, the intensity value of Co₃O₄ exhibits a tendency to decrease, which can be attributed to the coalescences of

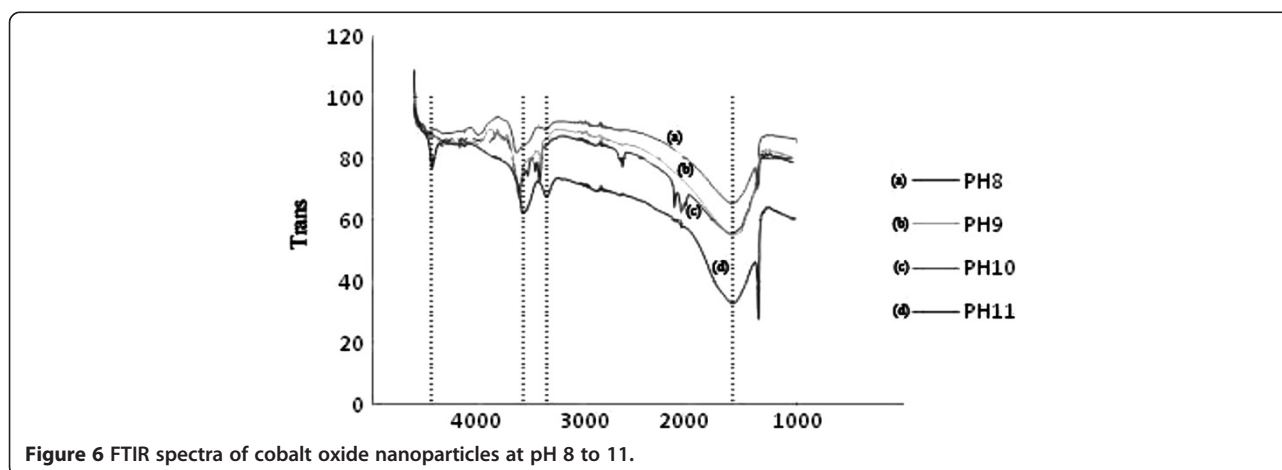


Figure 6 FTIR spectra of cobalt oxide nanoparticles at pH 8 to 11.

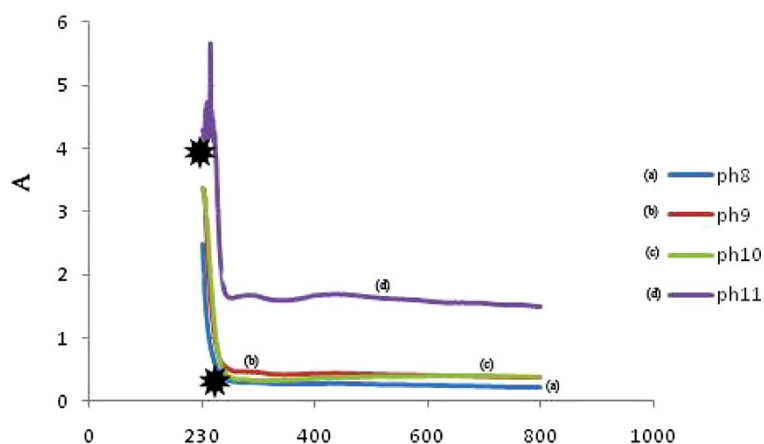


Figure 7 UV results of cobalt oxides at pH 8, 9, 10, and 11 from bottom to top.

grains at higher annealing temperature. As a result, it implies that the crystallinity of the Co_3O_4 is improved at higher annealing temperatures. This may be due to high annealing temperature providing energy to crystallites gaining enough energy to orient in proper equilibrium sites, resulting in the improvement of crystallinity and degree of orientation of the Co_3O_4 .

Figure 13a, b, c shows SEM images of cobalt annealed at 400°C , 500°C , and 600°C . The figure shows nearly the same surface morphology with slight increase in grain

size. The surface looks smooth and composed of very fine elongated particles smaller than 80 nm in length connected by two to three spherical grains of about 40 to 45 nm in diameters. From the SEM image, overgrowth of clusters is clearly seen. Initially grown. The percent of crystallization and related facts mentioned about SEM can be concluded from the images at Figure 14 and Figure 15 showing the EDX. Nanograins may have increased their size by further deposition and come closer to each other. The cobalt oxide surface is well

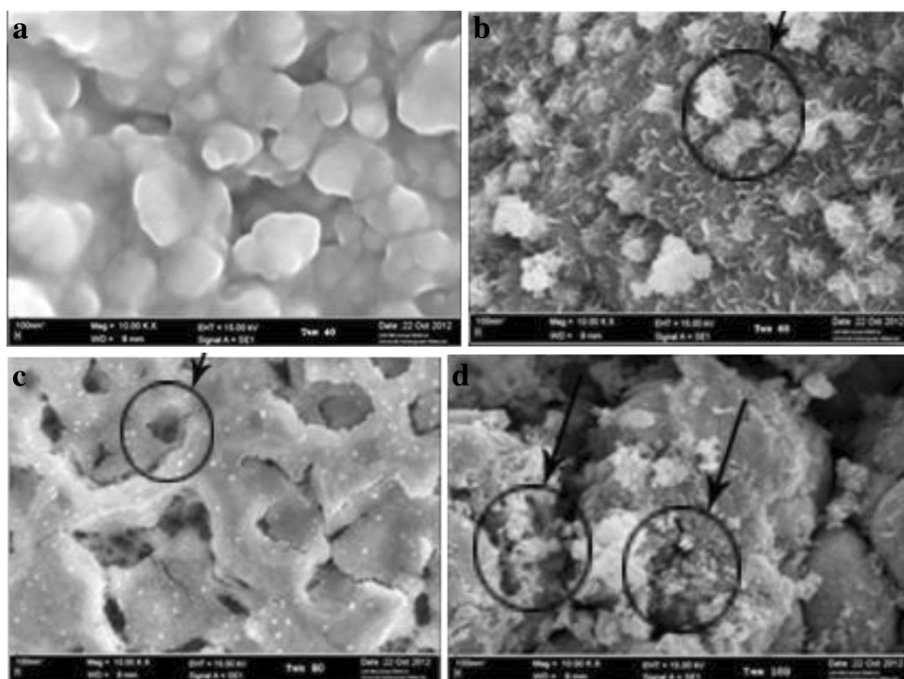


Figure 8 SEM images of cobalt oxides at temperatures of 40°C (a), 60°C (b), 80°C (c), and 100°C (d).

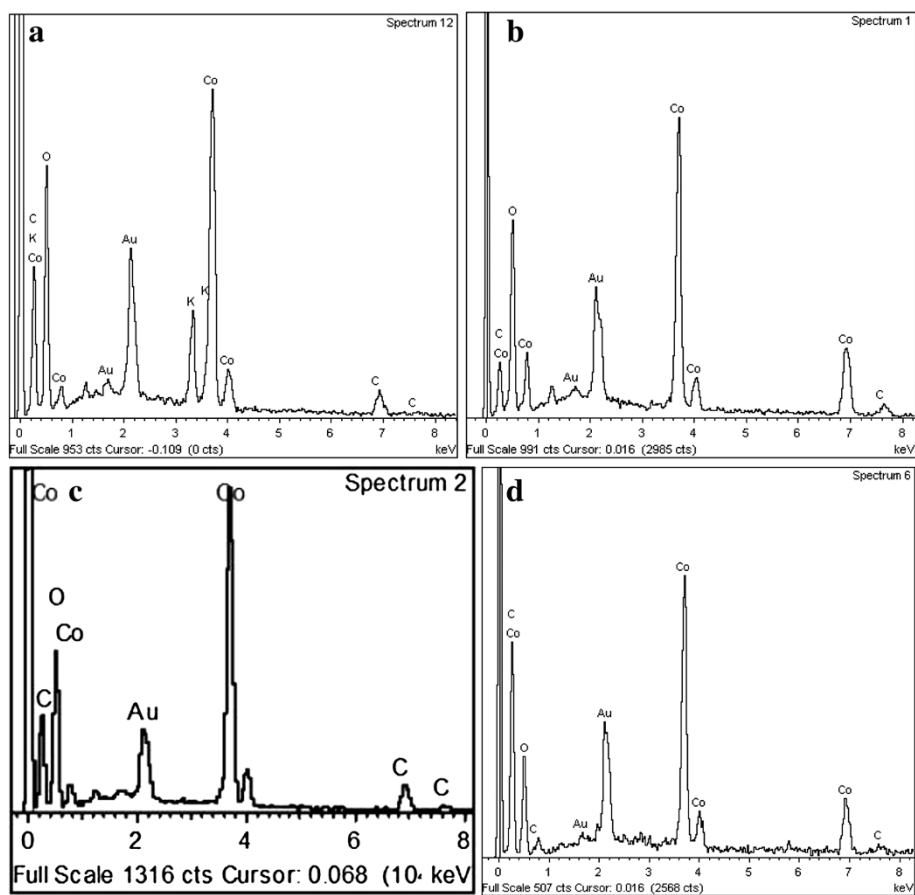


Figure 9 EDX spectra of cobalt oxides at temperatures of 40°C (a), 60°C (b), 80°C (c), and 100°C (d).

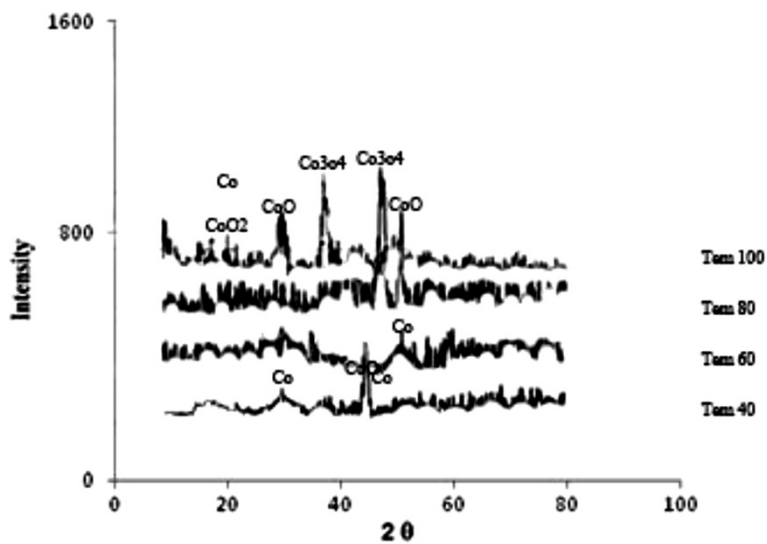


Figure 10 XRD patterns of samples synthesized at different temperatures: 40°C, 60°C, 80°C, and 100°C.

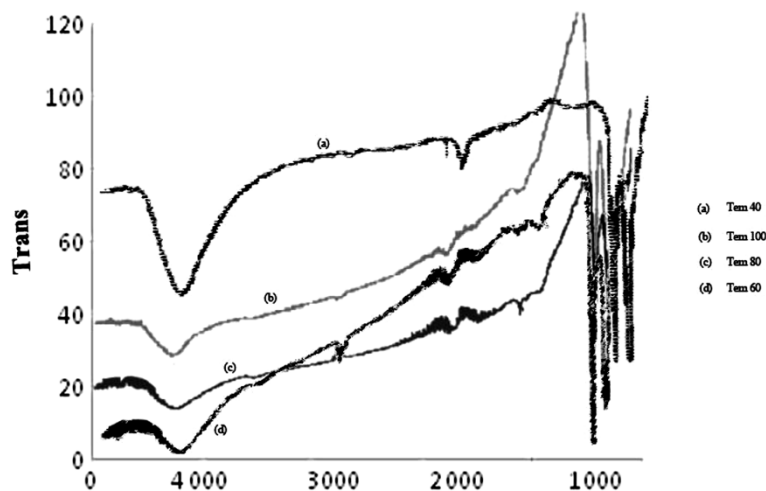


Figure 11 FTIR results of cobalt oxides at different synthesis temperatures.

covered without any pinholes and cracks. Such surface morphology may offer increased surface area.

Effect of capping agent

Fourier transform infrared spectroscopy (FTIR) is a powerful tool to study the capping of surfactants to the surface of the nanoparticles. Figure 16 shows the FTIR data for pure oleic acid and DDOA. The notable features of the spectrum in oleic acid are a band centered at $1,500\text{ cm}^{-1}$ and a peak occurring at $3,400\text{ cm}^{-1}$. We also observe bands positioned at $2,700$ and $1,070\text{ cm}^{-1}$ which are designated to

symmetric and anti-symmetric stretching of CoO. The most important differences in this spectrum from that of oleic acid are the shift in the band from $1,500$ to $1,100\text{ cm}^{-1}$ and the disappearance of the peak at $3,400\text{ cm}^{-1}$.

The FTIR spectrum for purified DDOA molecule is shown in Figure 16. The band at $1,737\text{ cm}^{-1}$ is assigned to C=O stretch, while the peaks appearing at $2,732$ and $3,000\text{ cm}^{-1}$ are assigned to symmetric and anti-symmetric stretching of CH_2 .

Here, the most prominent difference when this molecule is present on Co nanoparticle surface is the shift observed

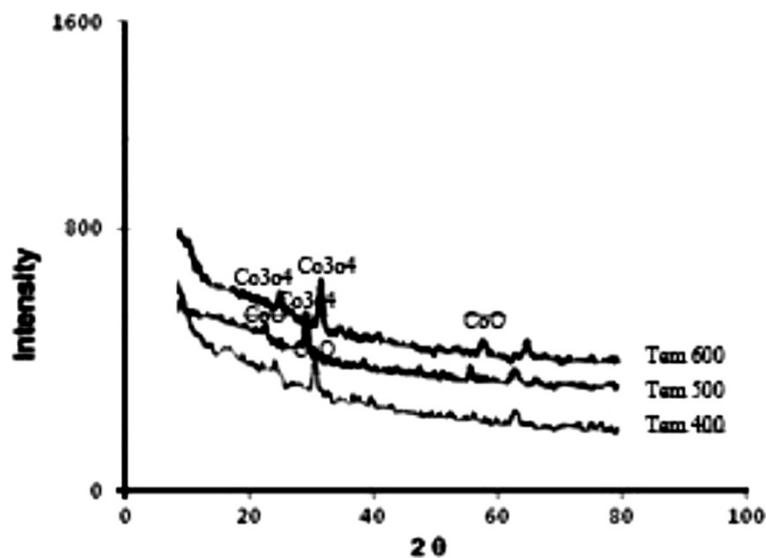


Figure 12 X-ray diffraction patterns of Co_3O_4 at different annealing temperatures.

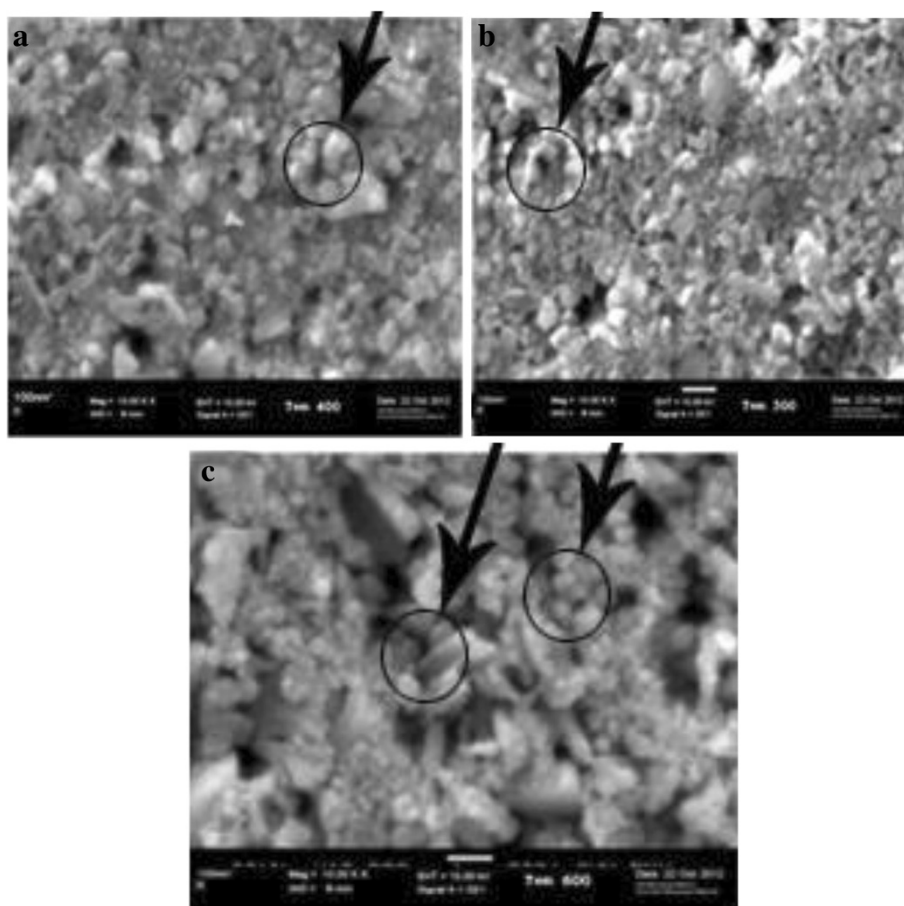


Figure 13 SEM images of cobalt oxides at annealing temperatures of 400°C (a), 500°C (b), and 600°C (c).

in the peak from $1,490$ to $1,300\text{ cm}^{-1}$. The pure oleic acid spectrum, peak positioned at $1,500\text{ cm}^{-1}$ is assigned to C=O stretch, while the peak occurring at $3,309\text{ cm}^{-1}$ represents the stretching of olefinic C-H. In the FTIR spectra of oleic acid-capped Co nanoparticles, a shift in peak corresponding to C=O is observed, while the peak corresponding to C=C-H stretch vanishes and also the peak occurring at $2,702\text{ cm}^{-1}$ corresponding to CoO. Disappearance of this peak indicates binding of double bond to the surface of nanoparticles, while the shift in C=O peak is due to carboxylate formation. Comparative FTIR study was carried out for OA-Co nanoparticles. We wish to highlight here that in the pure OA case, if the binding to the Co nanoparticles is through the double bond or carboxylic ends with Co nanoparticle surface, an unfavorable situation where $-\text{CH}_3$ end is exposed to aqueous environment would result. This could be the reason why oleic acid does not act as good capping agent in aqueous environment. In the case of

DDOA, binding to the surface of nanoparticles occurs only through the $-\text{COOH}$ group as it does not contain a double bond. This is indicated by the shift in peak. However, by changing appropriate precursors and organic transformation, changes to this ligand structure can be accomplished.

Figure 17 demonstrates the X-ray diffraction patterns for oleic acid. The as-prepared sample displays no features. Clear and distinguishable peaks are observed for Co_3O_4 , while high peaks are observed for CoO. The figure also demonstrates the X-ray diffraction pattern for DDOA-capped Co nanoparticles. In this case, the diffraction pattern was recorded for the powder sample heated at 300°C as no diffraction was observed for the as-prepared sample. The peak observed corresponds to the Co_3O_4 , and just two weak peaks correspond for CoO.

The particle size obtained with DDOA as capping agent was smaller than those obtained with oleic acid (Figure 18). The average sizes calculated using Scherrer's

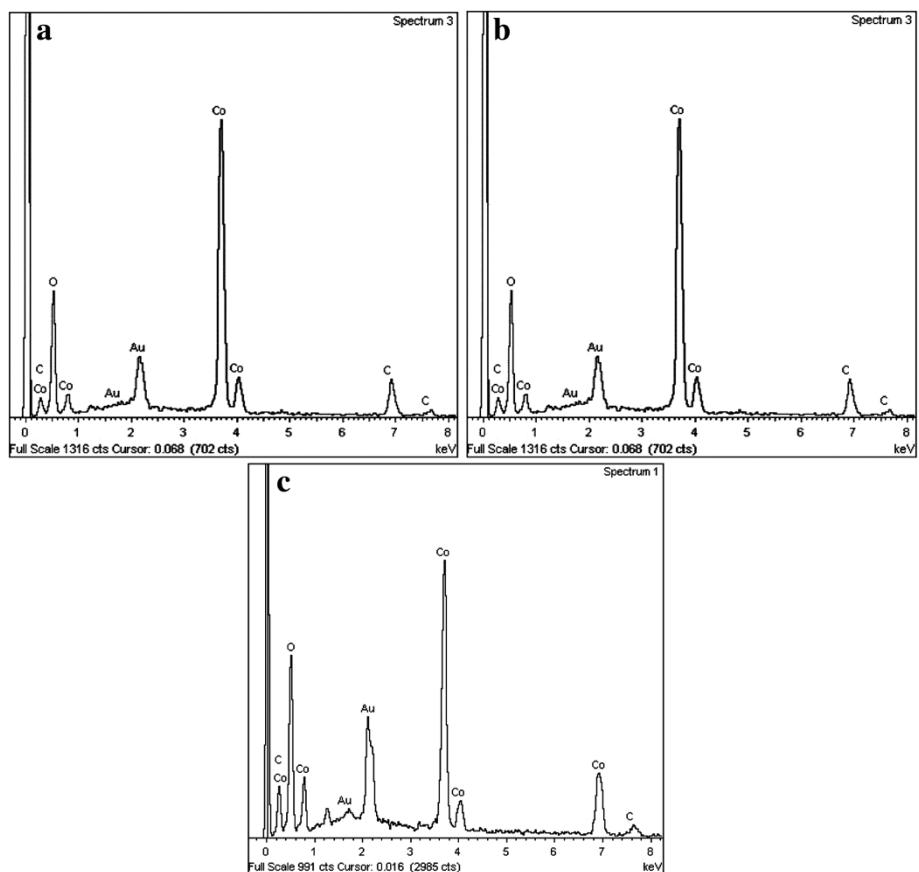


Figure 14 EDX spectra of cobalt oxides at annealing temperatures of 400°C (a), 500°C (b), and 600°C (c).

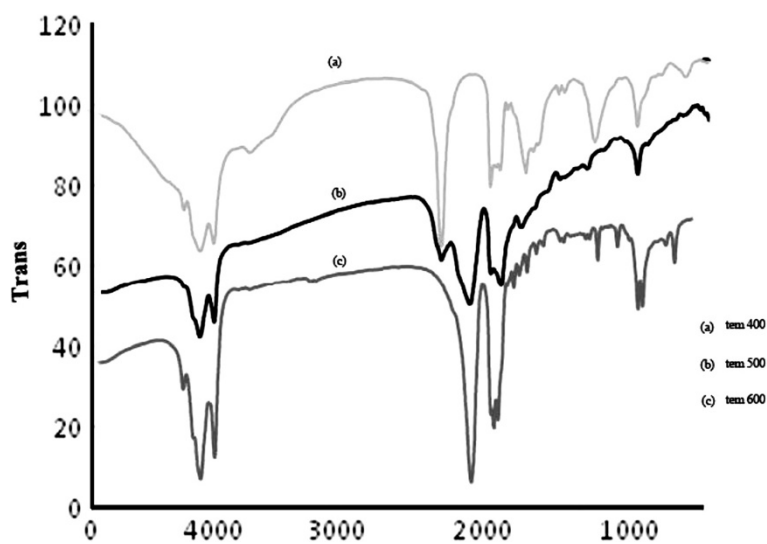


Figure 15 FTIR results of cobalt oxides at different annealing temperatures.

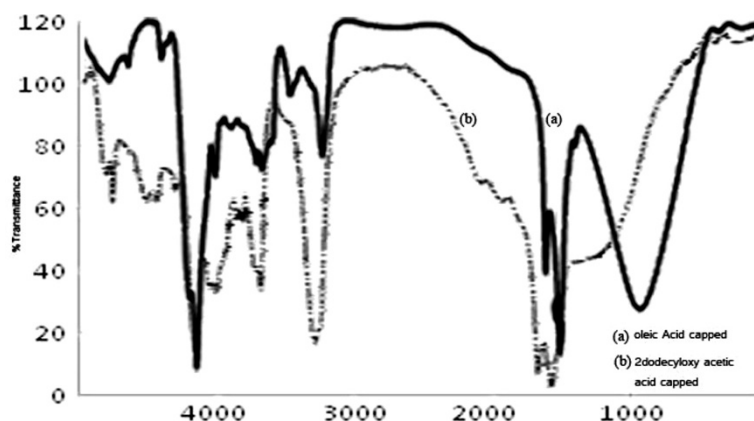


Figure 16 FTIR results of cobalt nanoparticles capped with oleic acid and DDOA.

formula were 35 and 45 nm for DDOA and oleic acid, respectively. SEM analysis carried out for oleic acid shows aggregated nanoparticles with larger particle size (Figure 19). The poor capping ability of oleic acid in water can be implicated for this observation as oleic acid cannot stabilize Co nanoparticles leading to coalescence of particles. From our studies, it is observed that ligands used in the syntheses play an important role in governing the crystal structure of cobalt nanoparticles.

Effect of cobalt salt type

Figure 20 shows the SEM images of Co_3O_4 using different cobalt salts. It can be seen from the figure that only

nanocube morphologies of Co_3O_4 are shown using $\text{Co}(\text{NO}_3)_2 \cdot 6\text{H}_2\text{O}$ as cobalt salt. For comparison, typical spherical Co_3O_4 and also nanocubic Co_3O_4 are obtained when the cobalt salts are $\text{CoSO}_4 \cdot 7\text{H}_2\text{O}$. It can be concluded that the morphologies of Co_3O_4 are closely dependent on the anion type in cobalt salts. In other words, the anion type in cobalt salt plays a key role in the morphology of Co_3O_4 .

Several precursors (cobalt nitrate and cobalt sulfate) were used (Figure 21). It suggests that reduction of cobalt (II) nitrate to cobalt is requiring lower energy than the cobalt sulfate. This demonstrates that pure cobalt nanoparticles can be synthesized from cobalt (II) nitrate

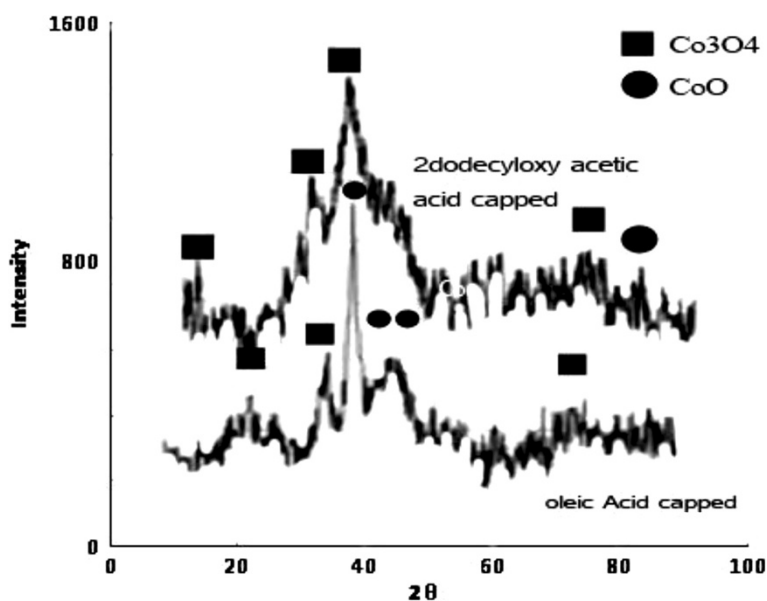


Figure 17 XRD spectra of oleic acid-capped cobalt nanoparticles and XRD patterns for as-prepared DDOA-capped cobalt nanoparticles.

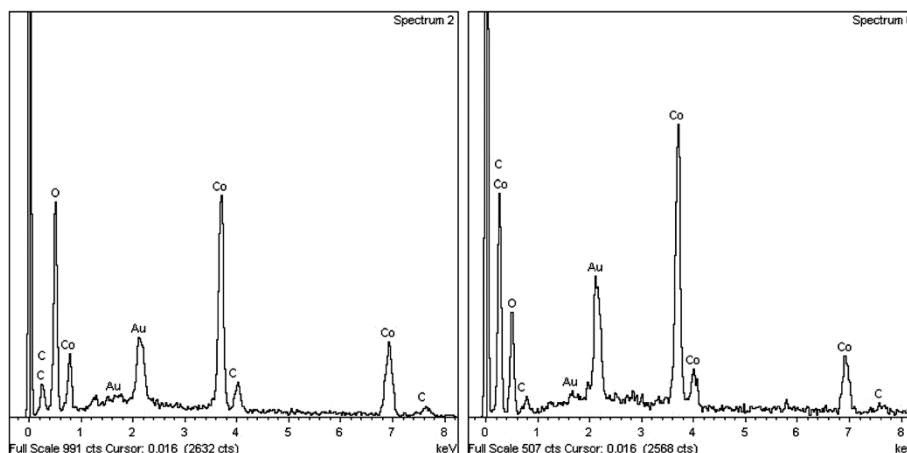


Figure 18 EDX spectra of cobalt nanoparticles with oleic acid (left) and DDOA (right) as capping agents.

as the removal of nitrates and water requires lower energy than the removal of water from cobalt sulfate. In addition, cobalt sulfate leaves carbon with the cobalt nanoparticles. XRD patterns of Co products prepared from nitrate and sulfate salts are shown in Figure 22. A broad peak at two angles between 40° and 50° ($2\theta = 42^\circ, 48.50^\circ, \text{ and } 50^\circ$) corresponds to Co_3O_4 materials. Co_3O_4 is the dominant crystalline species. Peaks representing residual or impurity (formed during nitrate decomposition) are not seen, indicating complete decomposition or removal after the washing procedure, but for sulfate, there is just one weak peak for CoO (Figure 23).

Conclusion

As a conclusion, we can say that Co_3O_4 with the average particle size of 40 nm is formed when pH is 8 to 9, and when pH increases at 10 to 11, irregular

Co_3O_4 with grains are seen and the size is averagely 30. Thus, pH has a great effect on the Co_3O_4 formation. To achieve the optimum pH, the other experiments were done. In the other experiment, two capping agents, DDOA and oleic acid, were used to see the result; particles with oleic acid are irregular in shape and are clustered. Particle size distribution indicates that the size of the particle is 35 nm. In addition to the mentioned factors, the cobalt salt also plays an important role. It can be concluded that the morphologies of Co_3O_4 are dependent on the anion type in cobalt salts. In other words, the anion type in cobalt salt plays a key role in the morphology of Co_3O_4 . The morphologies of Co_3O_4 show irregular nanocubes, 45 nm in size, using $\text{Co}(\text{NO}_3)_2 \cdot 6\text{H}_2\text{O}$ as cobalt salt. Also, in the experiment done to observe the effect of annealing temperature, it was concluded

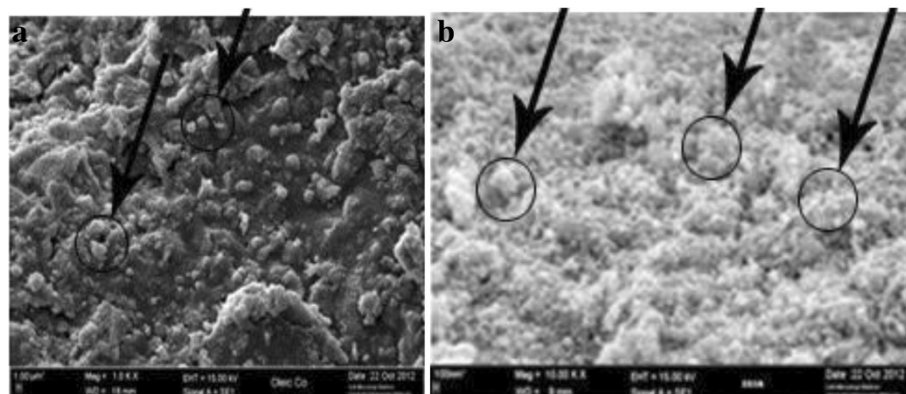


Figure 19 SEM images of cobalt nanoparticles with oleic acid (left) and DDOA (right) as capping agents.

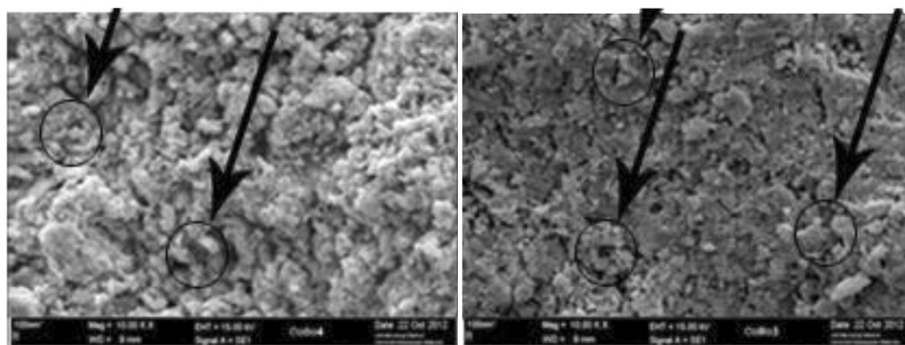


Figure 20 SEM images of CoSO_4 (left) and $\text{Co}(\text{NO}_3)_2$ (right) as cobalt salts.

that as the annealing temperature increases from 400°C to 600°C , the intensity value of Co_3O_4 exhibits a tendency to decrease, which can be attributed to the coalescences of grains at higher annealing temperature. As a result, it implies that the crystallinity of the Co_3O_4 is improved at higher annealing temperatures. In conclusion of observing the effect of heat of reaction, it was seen that when the reaction was performed at temperature lower than 60°C , the reaction rate was very slow and the prepared sample was amorphous and agglomerated. At temperatures higher than 60°C , the synthesis rate is fast, but the prepared samples showed that the higher temperature causes more agglomeration and amorphous percentage of samples that is increased because, at high reaction rate, nucleation and particle growth processes are not controllable.

Methods

All the materials were purchased from Sigma Aldrich (St. Louis, MO, USA) and Acros Organics (Geel, Belgium). In order to have the optimum pH to control the size and morphology of cobalt nanoparticles, the experiment was done. Thus, after the optimum pH was found, the other experiments were done with the selected pH. A 15 mmol cobalt salt ($\text{Co}(\text{NO}_3)_2 \cdot 6\text{H}_2\text{O}$) was dissolved into deionized water containing dispersant polyethylene glycol with relative molecular mass of about 20,000; then, excessive amount of NH_4OH was added with electromagnetic stirring at 50°C to form $\text{Co}(\text{OH})_2$ gel. The pH value was monitored at 8, 9, 10, and 11 by dropping KOH . A certain volume of 40% (mass fraction) H_2O_2 was dropped into the above suspension. Finally, the suspension was transferred into a centrifuge. Then, it was placed inside an oven to be heated at 100°C then cooled

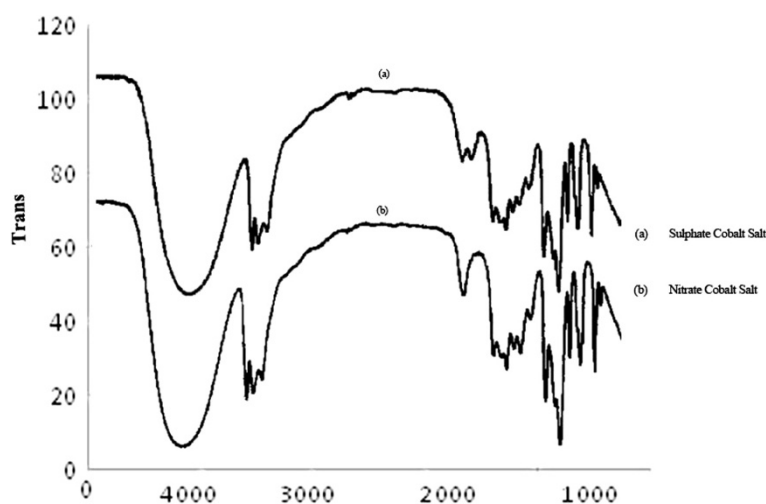


Figure 21 FTIR results of cobalt oxide with two cobalt types.

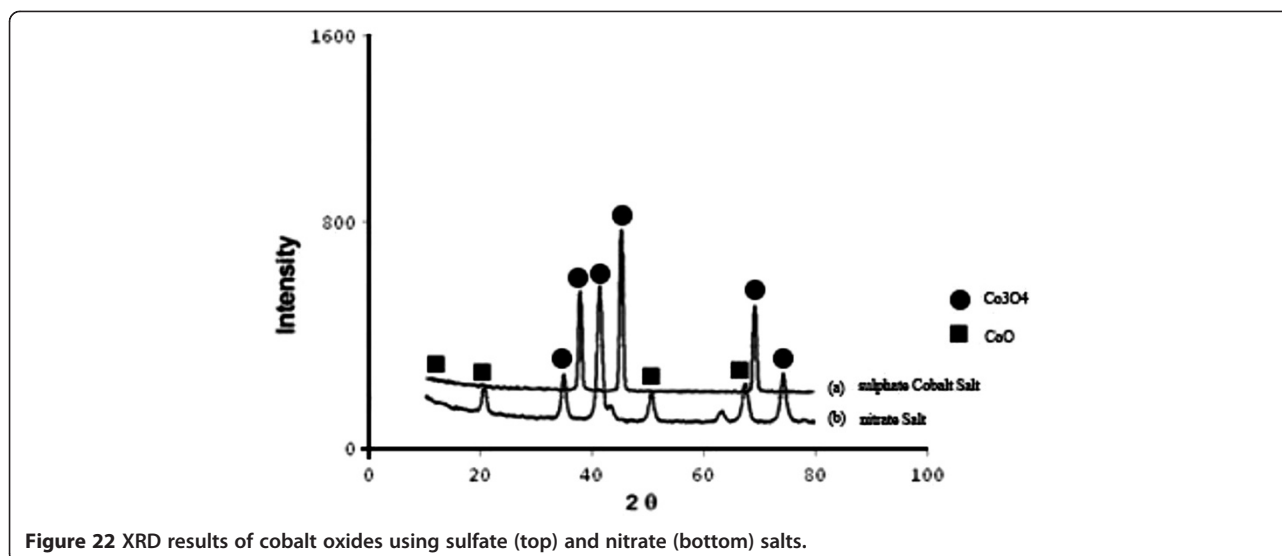


Figure 22 XRD results of cobalt oxides using sulfate (top) and nitrate (bottom) salts.

to room temperature in air naturally. The black products were centrifuged and washed with deionized water and ethanol for five times and then dried in a vacuum oven at 80°C for a day. The methods used to control pH are shown in Figure 24.

The methodology for other experiments is the same, but the factors have been changed such as synthesis temperature, annealing temperature, capping agent, and cobalt salts. In order to investigate the effect of synthesis temperature, the same procedure was done with pH 9 at four temperatures 40°C, 60°C, 80°C, and 100°C. In order to investigate the role of annealing temperature, the experiment was done as follows: Cobalt acetate tetrahydrate was added to 50 mL of methanol and stirred vigorously at 80°C for 1 h, leading to the formation

of light pink colored powder. Then, H₂O₂ was added to remove the black precipitate. The as-prepared powder was sintered at various temperatures ranging from 400°C, 500°C, to 600°C with a fixed annealing time of 1 h in an ambient air to obtain Co₃O₄ with different crystallite sizes. Another experiment was carried out to see the effect of capping agent. Synthesis of cobalt nanoparticles was carried using sodium borohydride (NaBH₄) as reducing agent. In a typical experiment, 100 mL of oleic acid was taken, and cobalt nitrite was added to this. This mixture was stirred for a day. Twenty milligrams of sodium borohydride was dissolved in 1 mL of deionized water and ethanol; since the oleic acid is insoluble, it was added to the mixture dropwise. On addition of NaBH₄, the color of the solution changed from light pink to black indicating

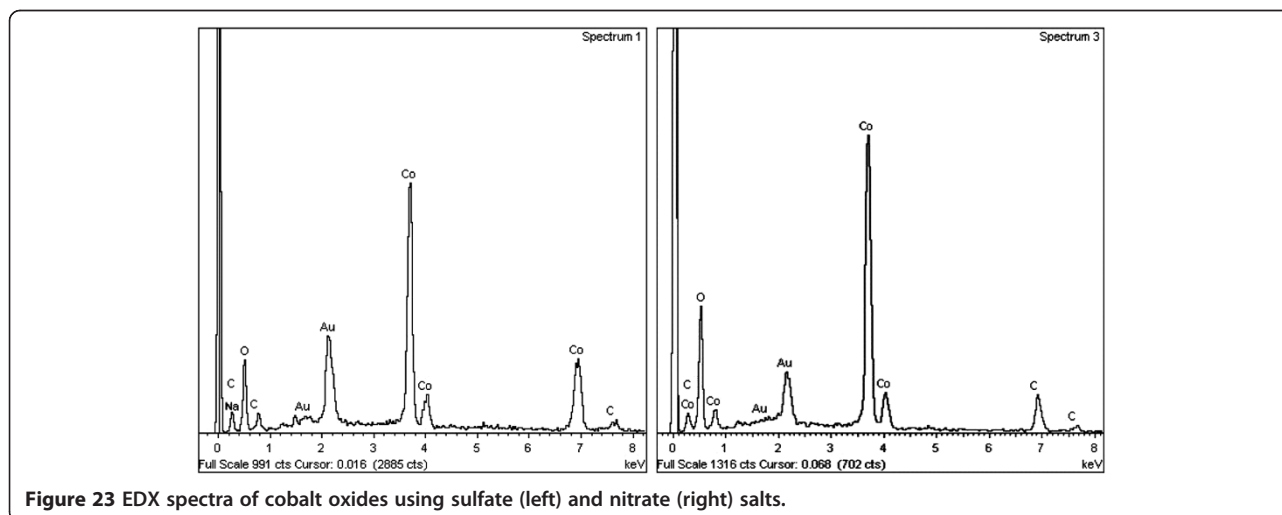


Figure 23 EDX spectra of cobalt oxides using sulfate (left) and nitrate (right) salts.

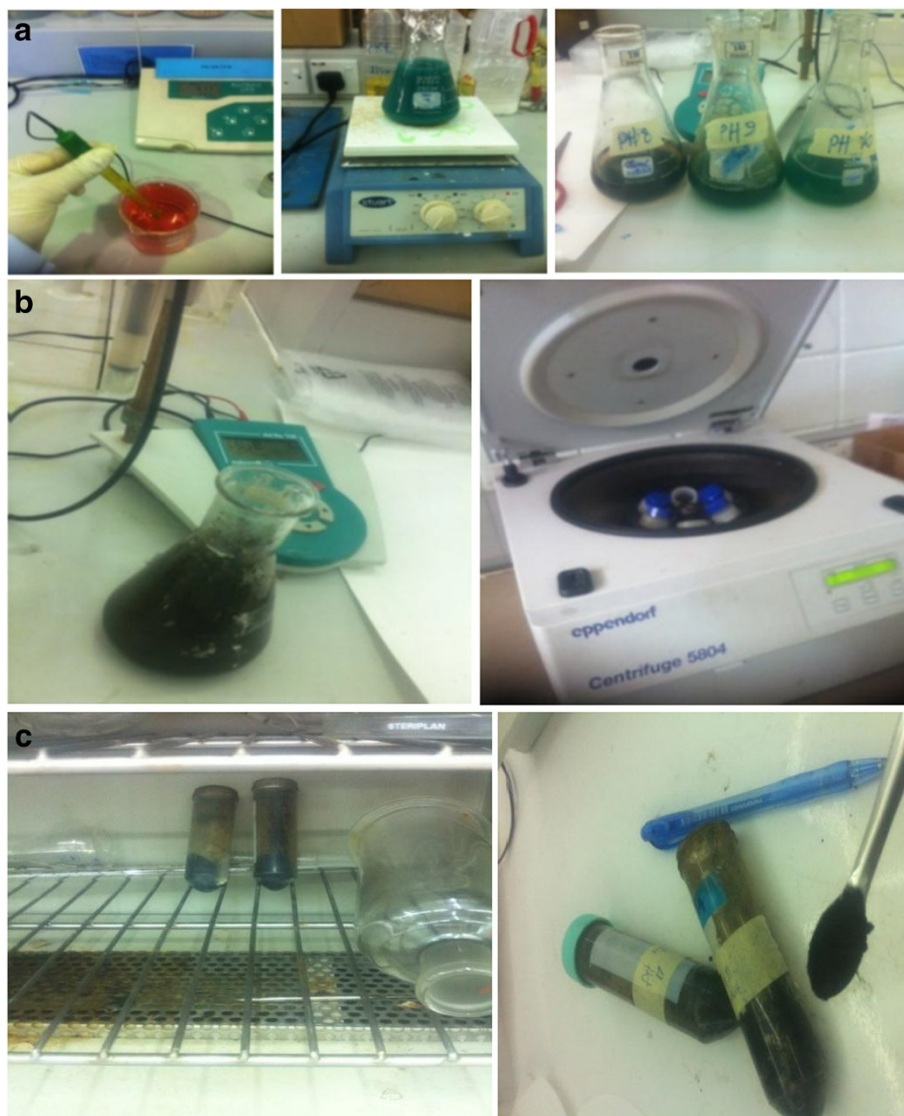


Figure 24 Methods used to control pH. (a) Stirring. (b) Centrifugation. (c) Heating and centrifugation.

the formation of cobalt nanoparticles. The nanoparticle solution was then centrifuged at 8,000 rpm for 20 min to remove uncoordinated surfactant and un-reacted NaBH_4 . The same experiment was carried out but using 2-(dodecyloxy) acetic acid (DDOA) as capping agent.

In order to see the effect of cobalt salt for obtaining Co_3O_4 powders, two cobalt salts were used. The precipitation agents, 0.1 M $\text{Co}(\text{NO}_3)_2$ solution and 0.2 M NH_3 solution, were added together to a 150 mL of water at a constant pH = 9 and at room temperature. The green precipitate was filtrated, washed, and dried at 110°C overnight and then calcined in air; the same procedure was done except for using cobalt sulfate as cobalt salt source. The sample was obtained from 0.5 M CoSO_4

solution and 0.2 M NH_3 solution as precipitating agent at pH = 9.5.

Characterization

To study the obtained products, conventional characterization techniques were applied, such as XRD, SAED, SEM, IR spectroscopy, and UV-vis spectroscopy.

Abbreviations

DDOA: 2-(dodecyloxy) acetic acid; SAED: Selected area electron diffraction; SEM: Scanning electron microscope.

Competing interests

Both authors declare that they have no competing interests.

Authors' contributions

GA with the supervision of MA carried the studies. All authors read and approved the final manuscript.

Acknowledgments

We would like to appreciate the fund from UKM chemical Engineering department.

Received: 15 May 2013 Accepted: 18 July 2013

Published: 04 Oct 2013

References

1. Dinega, DP, Bawendi, MG: Influence of iron oleate complex structure on iron oxide nanoparticle formation. *J Appl Physiol* **85**, 4325–4330 (1999)
2. Puentes, VF, Krishnan, KM, Alivisatos, AP: Synthesis, self-assembly, and magnetic behavior of a two-dimensional superlattice of single-crystal e-Co nanoparticles. *Appl Phys Lett* **78**, 2187–2189 (2001)
3. Hyeon, T: Synthesis of highly crystalline and monodisperse magnetite nanocrystallites without a size-selection process. *J Am Chem Soc* **123**, 12798–12801 (2001)
4. Sergeev, C, Gubin, SP, Yurkov, GY, Kataeva, NA, Kurnakov: Microgranules and nanoparticles on their surface, pp. 1536–1540. Russian Academy of Sciences, Leninskii (2005)
5. Kodama, RH: Magnetic nanoparticles. *J Magn Magn Mater* **200**, 359–372 (1999)
6. Balela, MDL: Synthesis and characterization of cobalt nano particles by liquid-phase reduction. Master's thesis. RS201.N35 B183, pp. pp 1–4. Universiti Sains, Malaysia (2008). 8–32
7. Berger, D, Morfin, F, Matei, J, Volta, C: Studies on synthesis and characterization of Co₃O₄ powders for CO oxidation. *J Optoelectron Adv Mat* **9**, 1540–1545 (2007)
8. Yang, YP, Liu, RS, Huang, KL, Wang, LP, Liu, SQ, Zeng, WW: Preparation and electrochemical performance of nanosized Co₃O₄ via hydrothermal method. *Trans Nonferrous Metals Society of China* **17**, 1083–1085 (2007)

10.1186/2193-8865-3-77

Cite this article as: Allaedini and Muhammad: Study of influential factors in synthesis and characterization of cobalt oxide nanoparticles. *Journal Of Nanostructure in Chemistry* 2013, 3:77

Submit your manuscript to a SpringerOpen[®] journal and benefit from:

- Convenient online submission
- Rigorous peer review
- Immediate publication on acceptance
- Open access: articles freely available online
- High visibility within the field
- Retaining the copyright to your article

Submit your next manuscript at ► springeropen.com